

EFFECT OF MICROSTRUCTURE ON FIBER/MATRIX INTERFACE CRACK GROWTH IN UD AND CROSS-PLY LAMINATES UNDER TENSILE LOADING

INSIGHTS FROM LINEAR ELASTIC FRACTURE MECHANICS

Luca Di Stasio^{1,2}, Janis Varna¹, Zoubir Ayadi²

¹ Division of Materials Science, Luleå University of Technology, Luleå, Sweden

²EEIGM & IJL, Université de Lorraine, Nancy, France

Grupo de Elasticidad y Resistencia de Materiales, ETSI Sevilla

Sevilla (ES) - September 26, 2019



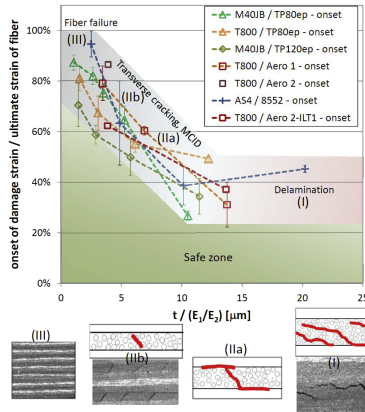
Outline

- ➔ Transverse Cracks Initiation
- ➔ Modeling
- ➔ Convergence
- ➔ Debond Initiation
- ➔ Debond Propagation

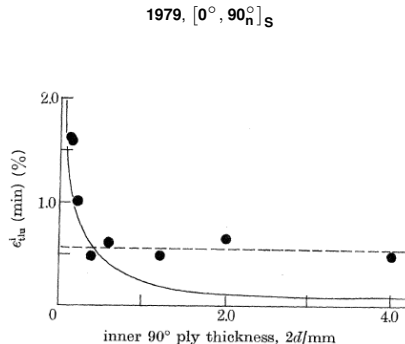
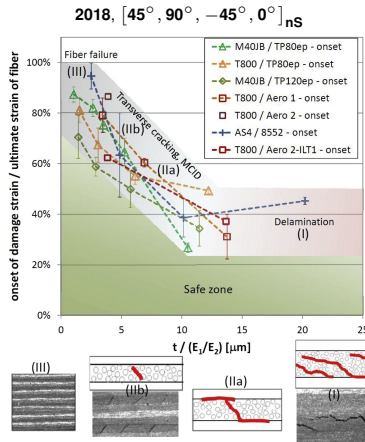
Transverse Cracks Initiation Modeling Convergence Debond Initiation Debond Propagation
The Thin-ply "Advantage" Micromechanics of Initiation

➔ TRANSVERSE CRACKS INITIATION

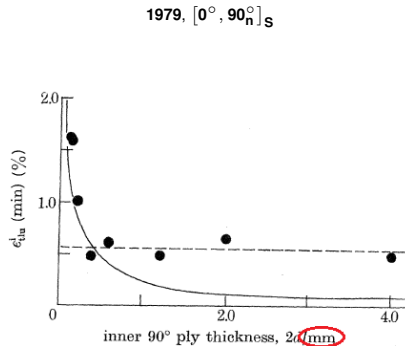
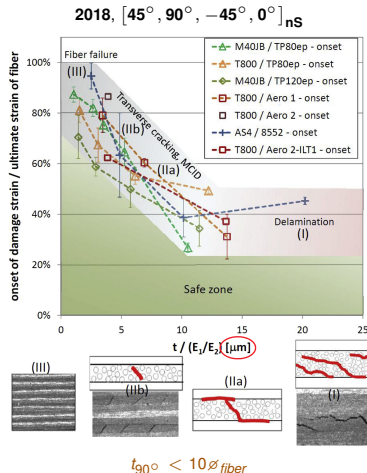
The Thin-ply "Advantage": new material

2018, $[45^\circ, 90^\circ, -45^\circ, 0^\circ]_{ns}$ Cugnoni et al., Compos. Sci. Technol. **168**, 2018.

The Thin-ply "Advantage": new material, old result



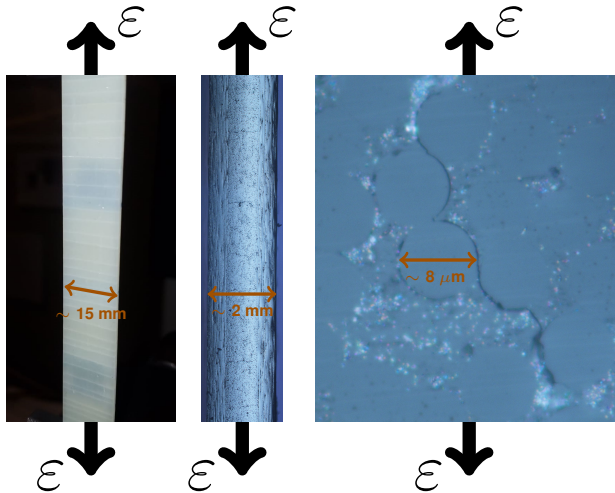
The Thin-ply "Advantage": new material, old result?



Cugnoni et al., Compos. Sci. Technol. **168**, 2018.

Bailey et al., P. Roy. Soc. A-Math. Phys. **366** (1727), 1979.

Micromechanics of Initiation



Left:
front view of $[0, 90_2]_S$,
visual inspection.

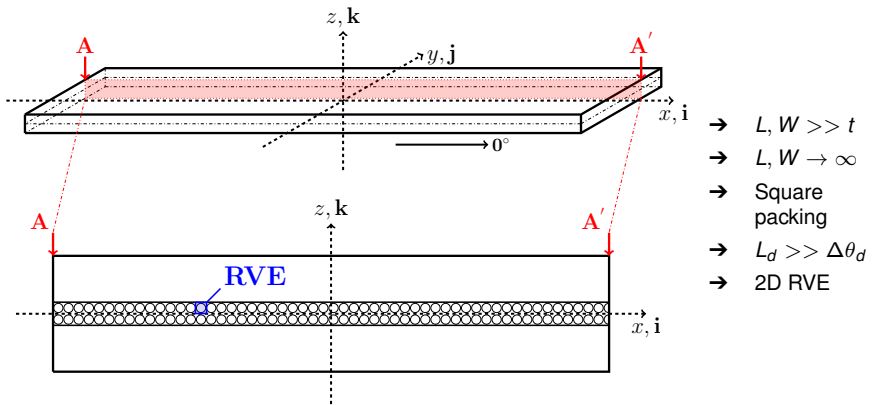
Center:
edge view of $[0, 90]_S$,
optical microscope.

Right:
edge view of $[0, 90]_S$,
optical microscope.

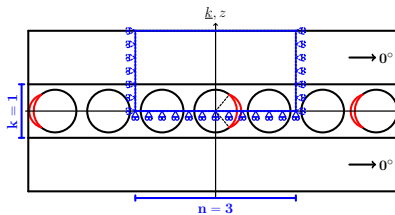
Transverse Cracks Initiation Modeling Convergence Debond Initiation Debond Propagation
Geometry Representative Volume Elements Assumptions Solution

MODELING

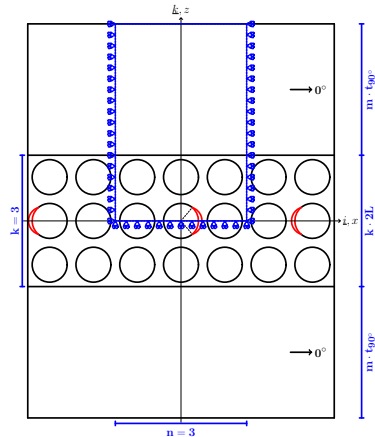
Geometry



Representative Volume Elements

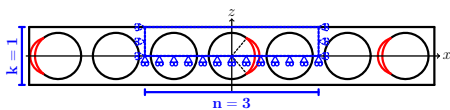


$$n \times 1 - m \cdot t_{90^\circ}$$

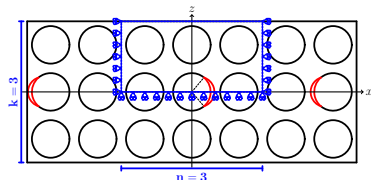


$$n \times k - m \cdot t_{90^\circ}$$

Representative Volume Elements

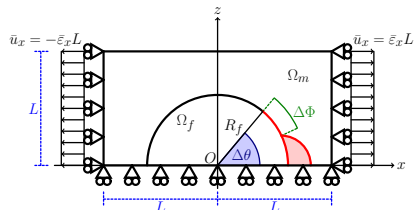


– free
 $n \times 1 - \text{coupling}$
– coupling + H



– free
 $n \times k - \text{coupling}$
– coupling + H

Assumptions

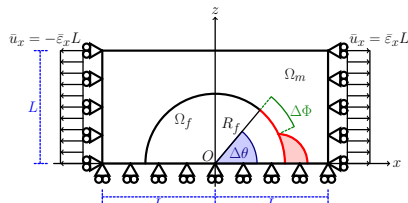


$$R_f = 1 \text{ } [\mu\text{m}] \quad L = \frac{R_f}{2} \sqrt{\frac{\pi}{V_f}}$$

- Linear elastic, homogeneous materials
- Concentric Cylinders Assembly with Self-Consistent Shear Model for UD
- Plane strain
- Frictionless contact interaction
- Symmetric w.r.t. x -axis
- Coupling of x -displacements on left and right side (repeating unit cell)
- Applied uniaxial tensile strain $\bar{\varepsilon}_x = 1\%$
- $V_f = 60\%$

Material	V_f [%]	E_L [GPa]	E_T [GPa]	μ_{LT} [GPa]	ν_{LT} [-]	ν_{TT} [-]
Glass fiber	-	70.0	70.0	29.2	0.2	0.2
Epoxy	-	3.5	3.5	1.25	0.4	0.4
UD	60.0	43.442	13.714	4.315	0.273	0.465

Solution



in Ω_f , Ω_m , Ω_{UD} :

$$\frac{\partial^2 \varepsilon_{xx}}{\partial z^2} + \frac{\partial^2 \varepsilon_{zz}}{\partial x^2} = \frac{\partial^2 \gamma_{zx}}{\partial x \partial z} \quad \text{for } 0^\circ \leq \alpha \leq \Delta\theta : \quad (\vec{u}_m(R_f, \alpha) - \vec{u}_f(R_f, \alpha)) \cdot \vec{n}_\alpha \geq 0$$

$$\varepsilon_y = \gamma_{xy} = \gamma_{yz} = 0 \quad \text{for } \Delta\theta \leq \alpha \leq 180^\circ :$$

$$\frac{\partial \sigma_{xx}}{\partial x} + \frac{\partial \tau_{zx}}{\partial z} = 0 \quad \vec{u}_m(R_f, \alpha) - \vec{u}_f(R_f, \alpha) = 0$$

$$\frac{\partial \tau_{zx}}{\partial x} + \frac{\partial \sigma_{zz}}{\partial z} = 0 \quad \sigma_{ij} = E_{ijkl} \varepsilon_{kl}$$

+ BC

$$\sigma_{yy} = \nu (\sigma_{xx} + \sigma_{zz})$$

$$\forall \Delta\theta \neq 0^\circ$$

→ oscillating singularity

$$\sigma \sim r^{-\frac{1}{2}} \sin(\varepsilon \log r), \quad V_f \rightarrow 0$$

$$\varepsilon = \frac{1}{2\pi} \log \left(\frac{1-\beta}{1+\beta} \right)$$

$$\beta = \frac{\mu_2(\kappa_1 - 1) - \mu_1(\kappa_2 - 1)}{\mu_2(\kappa_1 + 1) + \mu_1(\kappa_2 + 1)}$$

→ receding contact

$$\rightarrow \frac{G(R_{f,2})}{G(R_{f,1})} = \frac{R_{f,2}}{R_{f,1}}, \quad \frac{G(\bar{\varepsilon}_{x,2})}{G(\bar{\varepsilon}_{x,1})} = \frac{\bar{\varepsilon}_{x,2}^2}{\bar{\varepsilon}_{x,1}^2}$$

→ FEM + LEFM (VCCT)

→ regular mesh of quadrilaterals at the crack tip:

- $AR \sim 1, \quad \delta = 0.05^\circ$

$$\forall \Delta\theta$$

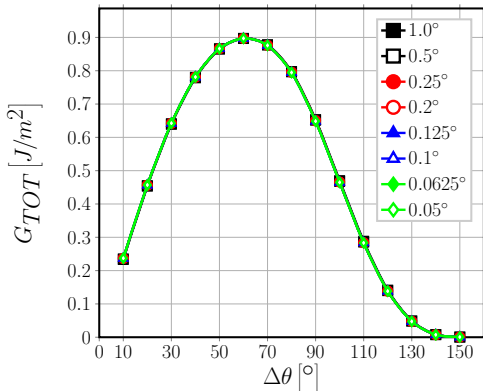
→ 2nd order shape functions

Transverse Cracks Initiation Modeling Convergence Debond Initiation Debond Propagation

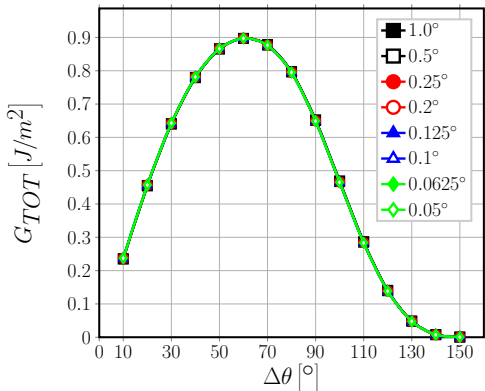
G_{TOT} G_I G_{II} Vectorial formulation of VCCT Asymptotic behavior Numerical convergence δ selection

CONVERGENCE

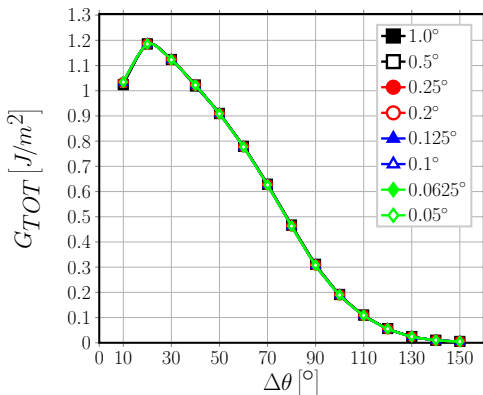
Transverse Cracks Initiation Modeling Convergence Debond Initiation Debond Propagation

 G_{TOT} G_I G_{II} Vectorial formulation of VCCT Asymptotic behavior Numerical convergence δ selection G_{TOT}  $\rightarrow 1 \times 1 - free, V_f = 0.1\%, 1^{st} \text{ order elements}$

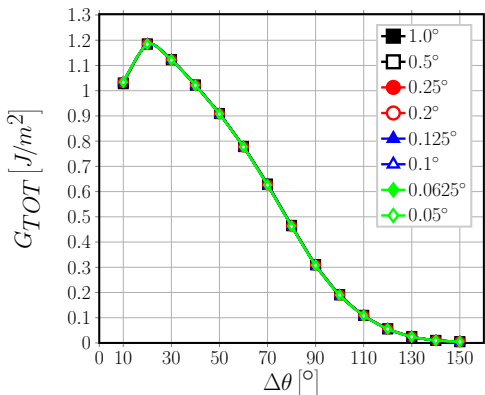
Transverse Cracks Initiation Modeling Convergence Debond Initiation Debond Propagation

 G_{TOT} G_I G_{II} Vectorial formulation of VCCT Asymptotic behavior Numerical convergence δ selection G_{TOT}  $\rightarrow 1 \times 1 - free, V_f = 0.1\%, 2^{nd} order elements$

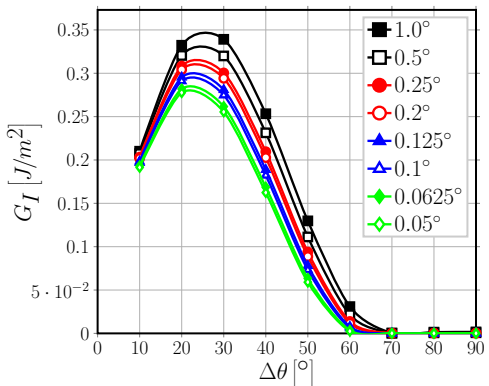
Transverse Cracks Initiation Modeling Convergence Debond Initiation Debond Propagation

 G_{TOT} G_I G_{II} Vectorial formulation of VCCT Asymptotic behavior Numerical convergence δ selection G_{TOT}  $\rightarrow 1 \times 1 - free, V_f = 40\%, 1^{st} order elements$

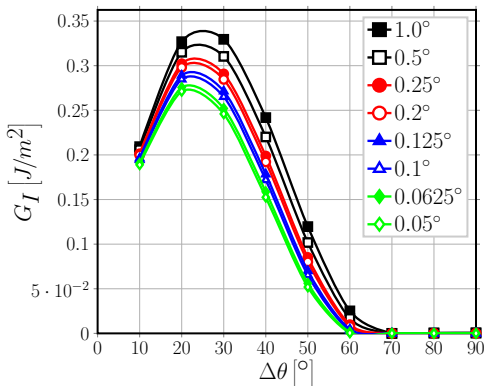
Transverse Cracks Initiation Modeling Convergence Debond Initiation Debond Propagation

 G_{TOT} G_I G_{II} Vectorial formulation of VCCT Asymptotic behavior Numerical convergence δ selection G_{TOT}  $\rightarrow 1 \times 1 - free, V_f = 40\%, 2^{nd} \text{ order elements}$

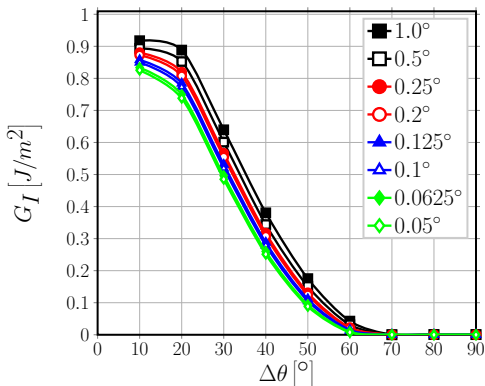
Transverse Cracks Initiation Modeling Convergence Debond Initiation Debond Propagation

 G_{TOT} G_I G_{II} Vectorial formulation of VCCT Asymptotic behavior Numerical convergence δ selection G_I  $\rightarrow 1 \times 1 - \text{free}, V_f = 0.1\%, 1^{\text{st}} \text{ order elements}$

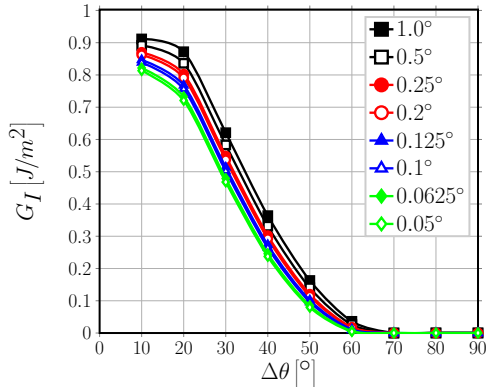
Transverse Cracks Initiation Modeling Convergence Debond Initiation Debond Propagation

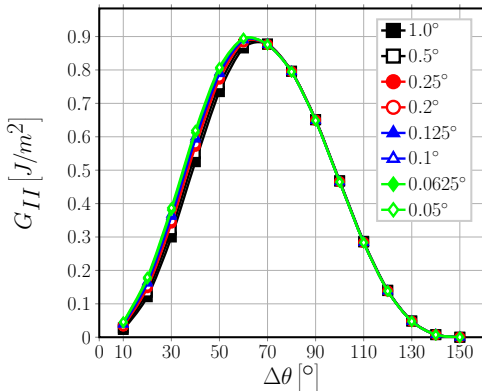
 G_{TOT} G_I G_{II} Vectorial formulation of VCCT Asymptotic behavior Numerical convergence δ selection G_I  $\rightarrow 1 \times 1 - free, V_f = 0.1\%, 2^{nd} \text{ order elements}$

Transverse Cracks Initiation Modeling Convergence Debond Initiation Debond Propagation

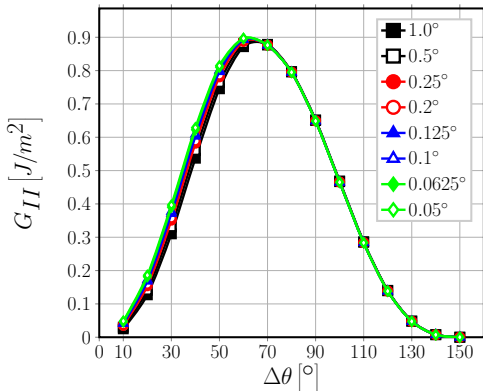
 G_{TOT} G_I G_{II} Vectorial formulation of VCCT Asymptotic behavior Numerical convergence δ selection G_I  $\rightarrow 1 \times 1 - free, V_f = 40\%, 1^{st} \text{ order elements}$

Transverse Cracks Initiation Modeling Convergence Debond Initiation Debond Propagation

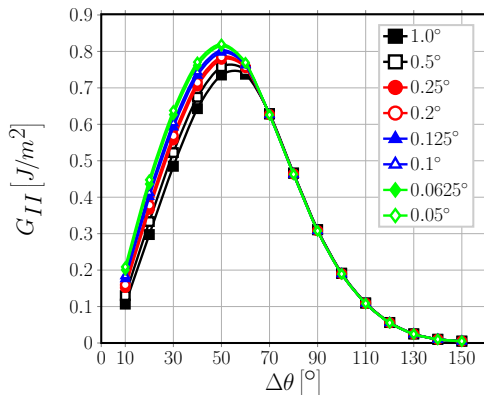
 G_{TOT} G_I G_{II} Vectorial formulation of VCCT Asymptotic behavior Numerical convergence δ selection G_I  $\rightarrow 1 \times 1 - free, V_f = 40\%, 2^{nd} \text{ order elements}$

G_{II}  $\rightarrow 1 \times 1 - free, V_f = 0.1\%, 1^{st} \text{ order elements}$

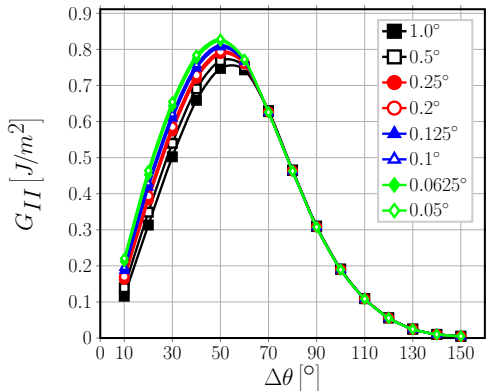
Transverse Cracks Initiation Modeling Convergence Debond Initiation Debond Propagation

 G_{TOT} G_I G_{II} Vectorial formulation of VCCT Asymptotic behavior Numerical convergence δ selection G_{II}  $\rightarrow 1 \times 1 - free, V_f = 0.1\%, 2^{nd} \text{ order elements}$

Transverse Cracks Initiation Modeling Convergence Debond Initiation Debond Propagation

 G_{TOT} G_I G_{II} Vectorial formulation of VCCT Asymptotic behavior Numerical convergence δ selection G_{II}  $\rightarrow 1 \times 1 - free, V_f = 40\%, 1^{st} order elements$

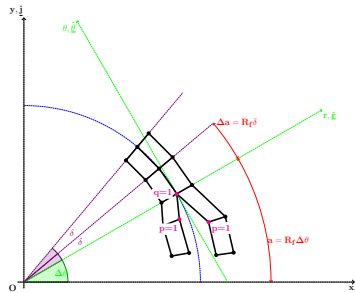
Transverse Cracks Initiation Modeling Convergence Debond Initiation Debond Propagation

 G_{TOT} G_I G_{II} Vectorial formulation of VCCT Asymptotic behavior Numerical convergence δ selection G_{II}  $\rightarrow 1 \times 1 - free, V_f = 40\%, 2^{nd} \text{ order elements}$

Transverse Cracks Initiation Modeling Convergence Debond Initiation Debond Propagation

G_{TOT} G_I G_{II} Vectorial formulation of VCCT Asymptotic behavior Numerical convergence δ selection

Vectorial formulation of VCCT

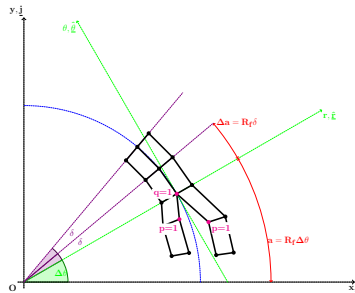


$$G_{TOT} = \frac{1}{2R_f\delta} \sum_{p=1}^{m+1} \sum_{q=1}^{m+1} Tr \left(Q \underline{\underline{R}}_{\underline{\underline{\delta}}=\Delta\theta} \underline{\underline{K}}_{xy,q} \underline{u}_{xy,q}^T \underline{\underline{u}}_{xy,p} \underline{\underline{R}}_{\underline{\underline{\Delta\theta}}=\delta}^T \underline{\underline{P}}_{pq}^T \underline{\underline{T}}_{pq}^T \right) + \\ + \frac{1}{2R_f\delta} \sum_{p=1}^{m+1} \sum_{q=1}^{m+1} Tr \left(Q \underline{\underline{R}}_{\underline{\underline{\Delta\theta}}=\Delta\theta} \widetilde{\underline{\underline{F}}}_{xy,q} \underline{u}_{xy,p}^T \underline{\underline{R}}_{\underline{\underline{\Delta\theta}}=\delta}^T \underline{\underline{P}}_{pq}^T \underline{\underline{T}}_{pq}^T \right)$$

Transverse Cracks Initiation Modeling Convergence Debond Initiation Debond Propagation

G_{TOT} G_I G_{II} Vectorial formulation of VCCT Asymptotic behavior Numerical convergence δ selection

Vectorial formulation of VCCT



$$\begin{aligned} G = \begin{bmatrix} G_I \\ G_{II} \end{bmatrix} &= \frac{1}{2R_f \delta} \sum_{p=1}^{m+1} \sum_{q=1}^{m+1} \text{Diag} \left(Q_{\delta=\Delta\theta} R_{\delta=\Delta\theta} K_{xy,q} u_{xy,q}^T u_{xy,p} R_{\delta=\Delta\theta}^T P_{\delta=\delta}^T T_{pq}^T \right) + \\ &+ \frac{1}{2R_f \delta} \sum_{p=1}^{m+1} \sum_{q=1}^{m+1} \text{Diag} \left(Q_{\delta=\Delta\theta} R_{\delta=\Delta\theta} \tilde{K}_{N,q} u_N u_{xy,p}^T R_{\delta=\Delta\theta}^T P_{\delta=\delta}^T T_{pq}^T \right) \end{aligned}$$

Transverse Cracks Initiation Modeling Convergence Debond Initiation Debond Propagation

 G_{TOT} G_I G_{II} Vectorial formulation of VCCT Asymptotic behavior Numerical convergence δ selection

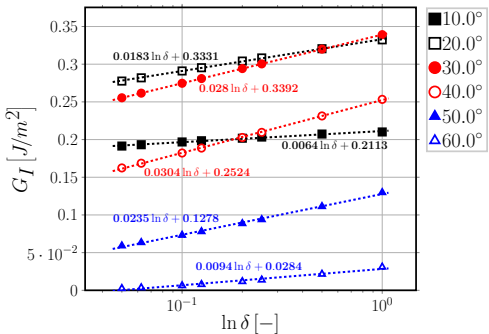
Asymptotic behavior

$$\frac{\partial \underline{G}}{\partial \delta} = \frac{1}{\delta} \underline{G} + \frac{1}{2R_f \delta} (\dots)$$

$$u(\delta) \sim \sqrt{\delta} (\sin, \cos)(\epsilon \log \delta) \quad \text{with} \quad \epsilon = \frac{1}{2\pi} \log \left(\frac{1-\beta}{1+\beta} \right)$$

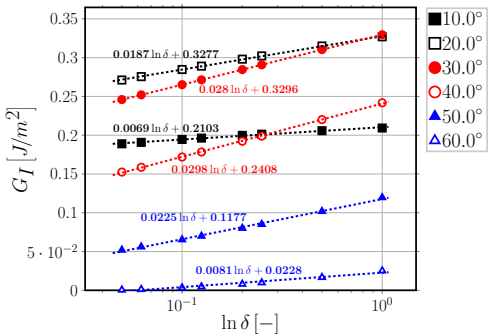
$$\lim_{\delta \rightarrow 0} \frac{\partial \underline{G}}{\partial \delta} \sim \frac{1}{\delta} \xrightarrow{\int d\delta} \lim_{\delta \rightarrow 0} \underline{G} \sim \underline{A} \log(\delta) + \underline{B}.$$

Numerical convergence: G_I



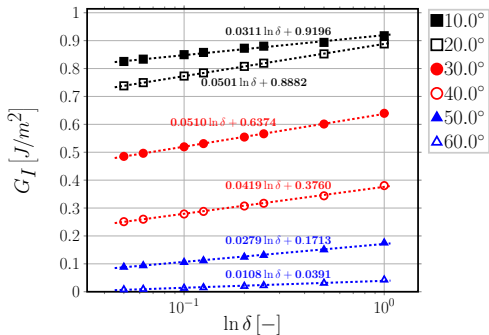
$\rightarrow 1 \times 1 - free, V_f = 0.1\%, 1^{st} order elements$

Numerical convergence: G_I



$\rightarrow 1 \times 1 - \text{free}, V_f = 0.1\%, 2^{\text{nd}} \text{ order elements}$

Numerical convergence: G_I

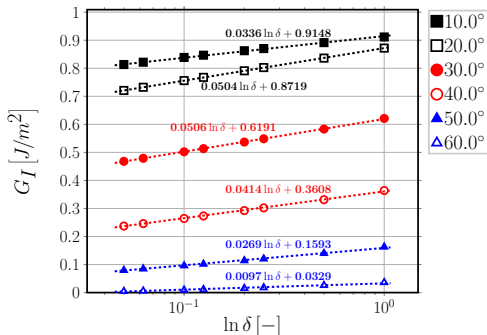


$\rightarrow 1 \times 1 - free, V_f = 40\%, 1^{st} order elements$

Transverse Cracks Initiation Modeling Convergence Debond Initiation Debond Propagation

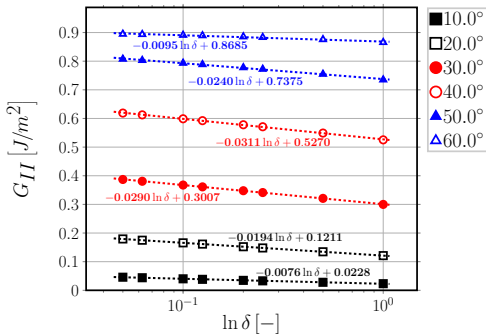
 G_{TOT} G_I G_{II} Vectorial formulation of VCCT Asymptotic behavior Numerical convergence δ selection

Numerical convergence: G_I



$\rightarrow 1 \times 1 - free, V_f = 40\%, 2^{nd} order elements$

Numerical convergence: G_{II}

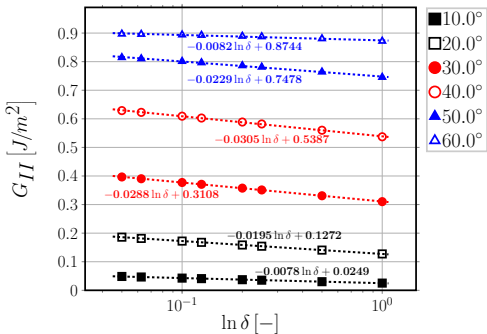


$\rightarrow 1 \times 1 - free, V_f = 0.1\%, 1^{st} order elements$

Transverse Cracks Initiation Modeling Convergence Debond Initiation Debond Propagation

 G_{TOT} G_I G_{II} Vectorial formulation of VCCT Asymptotic behavior Numerical convergence δ selection

Numerical convergence: G_{II}

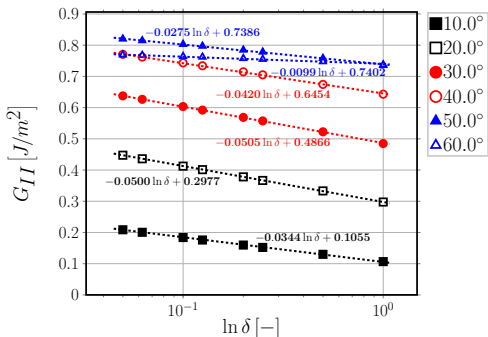


$\rightarrow 1 \times 1 - free, V_f = 0.1\%, 2^{nd} \text{ order elements}$

Transverse Cracks Initiation Modeling Convergence Debond Initiation Debond Propagation

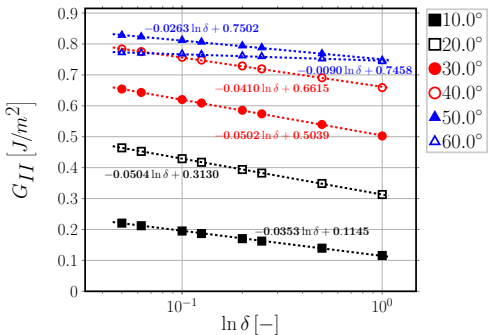
 G_{TOT} G_I G_{II} Vectorial formulation of VCCT Asymptotic behavior Numerical convergence δ selection

Numerical convergence: G_{II}



$\rightarrow 1 \times 1 - free, V_f = 40\%, 1^{st} order elements$

Numerical convergence: G_{II}

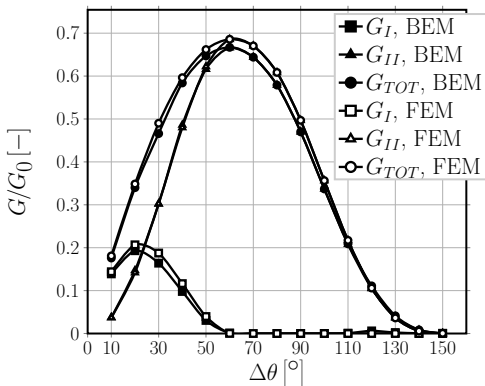


$\rightarrow 1 \times 1 - \text{free}, V_f = 40\%, 2^{\text{nd}} \text{ order elements}$

Transverse Cracks Initiation Modeling Convergence Debond Initiation Debond Propagation

 G_{TOT} G_I G_{II} Vectorial formulation of VCCT Asymptotic behavior Numerical convergence δ selection

δ selection



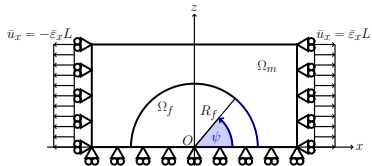
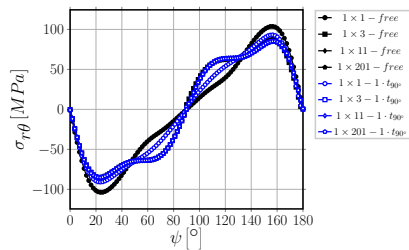
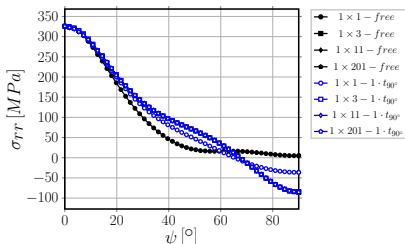
$\rightarrow 1 \times 1 - free, V_f = 0.01\%, 2^{nd} \text{ order elements}, \delta = 0.05^\circ$

Transverse Cracks Initiation Modeling Convergence Debond Initiation Debond Propagation

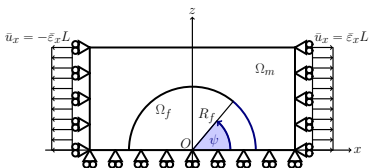
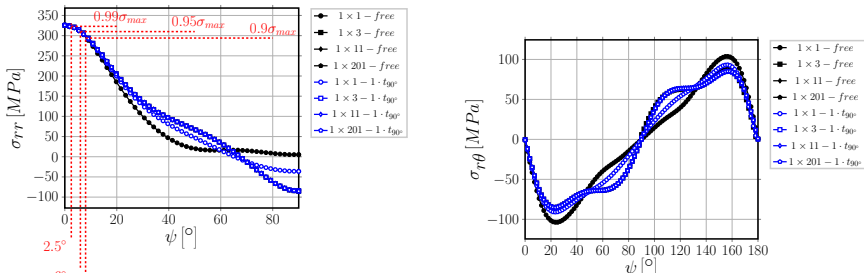
σ_{rr} vs $\tau_{r\theta}$ σ_{LHS} σ_{vM} σ_I Observations & Conclusions

DEBOND INITIATION

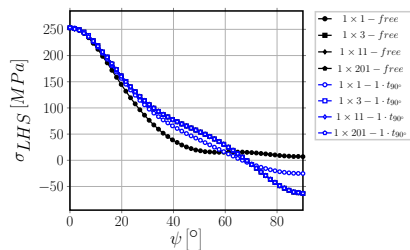
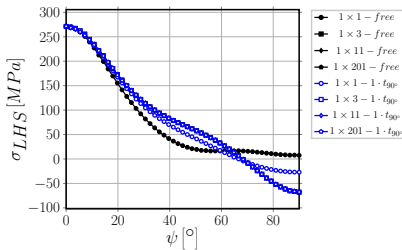
σ_{rr} vs $\tau_{r\theta}$: radial stress vs tangential shear at the interface



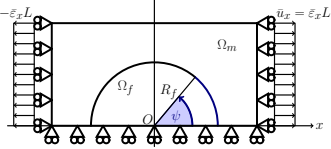
σ_{rr} vs $\tau_{r\theta}$: radial stress vs tangential shear at the interface



σ_{LHS} : local hydrostatic stress at the interface

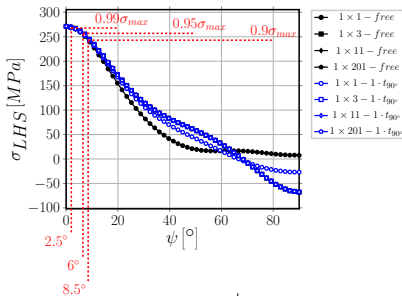


$$\sigma_{LHS}^{2D} = \frac{\sigma_{rr} + \sigma_{\theta\theta}}{2}$$

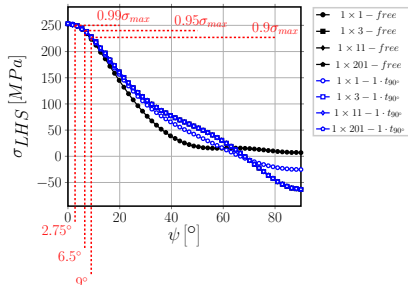
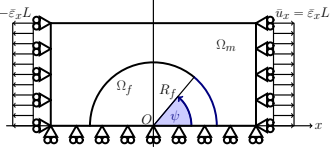


$$\sigma_{LHS}^{3D} = \frac{\sigma_{rr} + \sigma_{\theta\theta} + \sigma_{yy}}{3}$$

σ_{LHS} : local hydrostatic stress at the interface

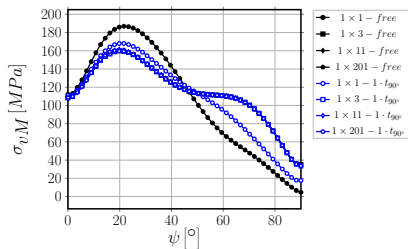
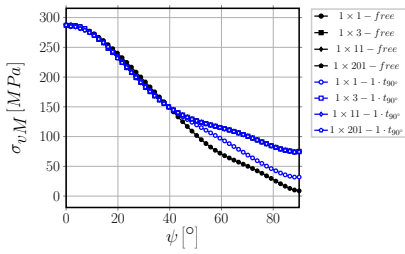


$$\sigma_{LHS}^{2D} = \frac{\sigma_{rr} + \sigma_{\theta\theta}}{2}$$



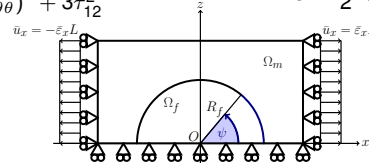
$$\sigma_{LHS}^{3D} = \frac{\sigma_{rr} + \sigma_{\theta\theta} + \sigma_{yy}}{3}$$

σ_{vM} : von Mises stress at the interface

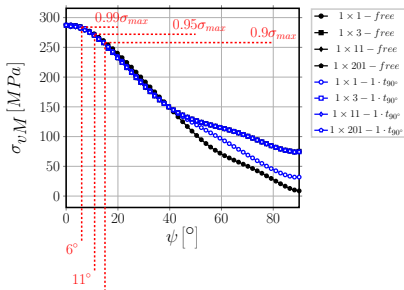


$$\sigma_{vM}^{2D} = \sqrt{(\sigma_{rr} - \sigma_{\theta\theta})^2 + 3\tau_{12}^2}$$

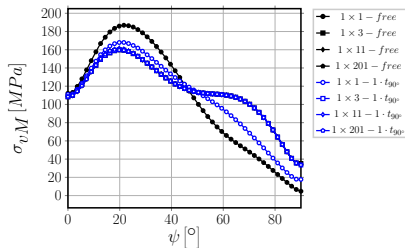
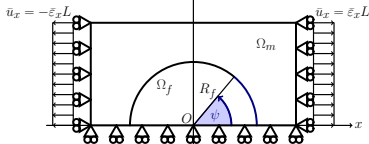
$$\sigma_{LHS}^{3D} = \frac{3}{2} s_{ij} s_{ij} \quad s_{ij} = \sigma_{ij} - \frac{1}{3} \sigma_{kk} \delta_{ij}$$



σ_{vM} : von Mises stress at the interface

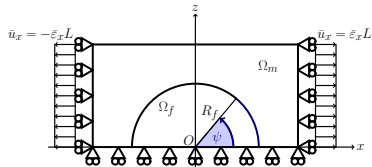
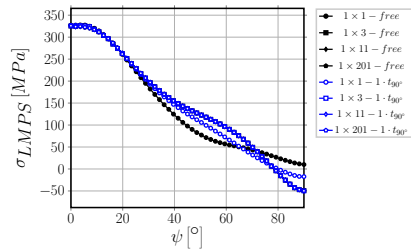
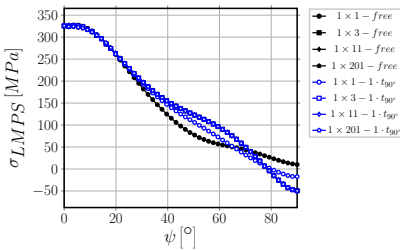


$$\sigma_{vM}^{2D} = \sqrt{(\sigma_{rr} - \sigma_{\theta\theta})^2 + 3\tau_{12}^2}$$

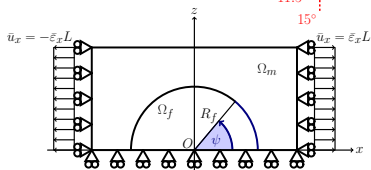
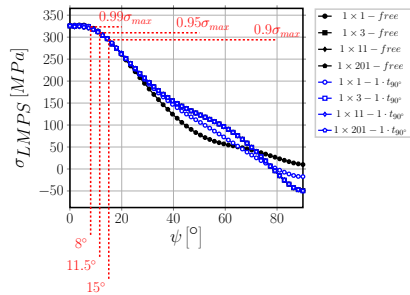
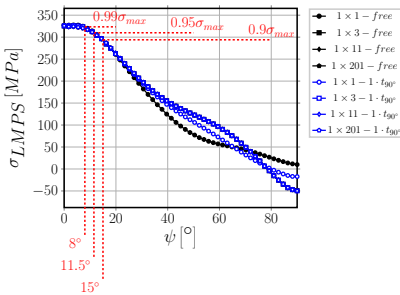


$$\sigma_{LHS}^{3D} = \frac{3}{2} s_{ij} s_{ij} \quad s_{ij} = \sigma_{ij} - \frac{1}{3} \sigma_{kk} \delta_{ij}$$

σ_I : maximum principal stress at the interface



σ_I : maximum principal stress at the interface



Observations & Conclusions

- For all stresses analyzed, no significant difference is present between the different RUCs for $\psi \leq 10^\circ$;
- for all stresses analyzed, no difference can be observed by increasing k when $k \geq 3$;
- for all stresses analyzed, no difference can be observed between $1 \times k - \text{free}$ and $1 \times k - 1 \cdot t_{90^\circ}$ for $k \geq 3$;
- σ_{rr} , $\sigma_{LHS,2D}$, $\sigma_{LHS,3D}$, $\sigma_{vM,2D}$, $\sigma_{LMPS,2D}$ and $\sigma_{LMPS,3D}$ all reach their peak value at 0° and 180° and decrease to 99% the peak value between 2° and 8° , to 95% the peak value between 6° and 12° and to 90% the peak value between 8° and 15° from the occurrence of the maximum.

It seems reasonable to conclude that...

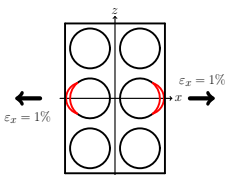
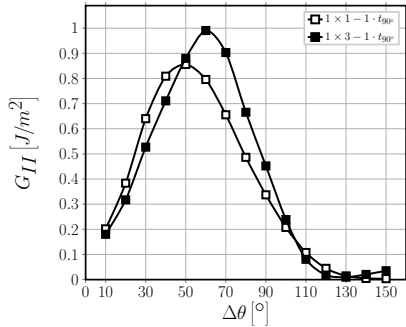
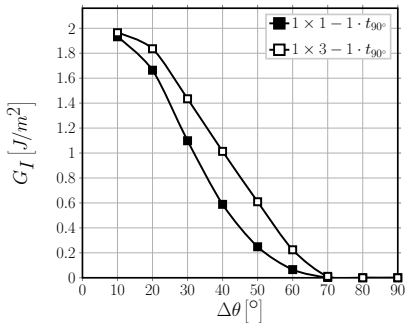
...a stress-based criterion would predict, irrespectively of the specific criterion chosen, the onset of an interface crack at 0° or 180° with an initial size at least comprised in the range $2^\circ - 8^\circ$ (1% margin) and likely in the range $6^\circ - 12^\circ$ (5% margin). Thus, no evident effect of 90° or 0° layer thickness can be observed.

Transverse Cracks Initiation Modeling Convergence Debond Initiation Debond Propagation

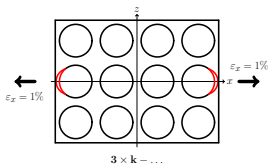
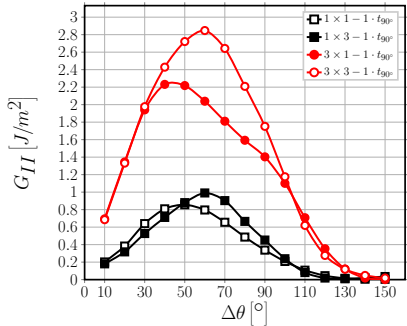
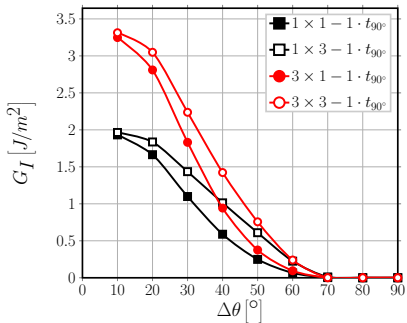
Interaction of Debonds Effect of 0° ply thickness Effect of 90° ply thickness Observations & Conclusions

DEBOND PROPAGATION

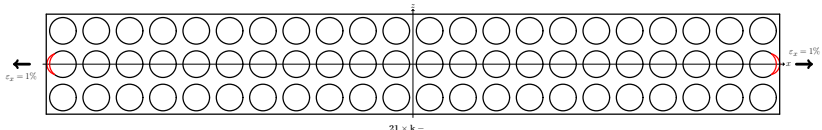
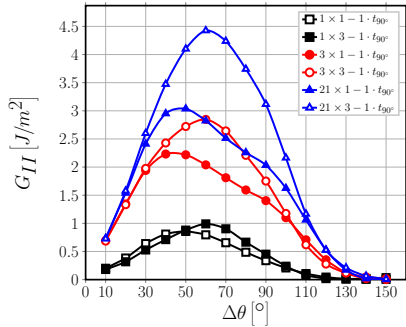
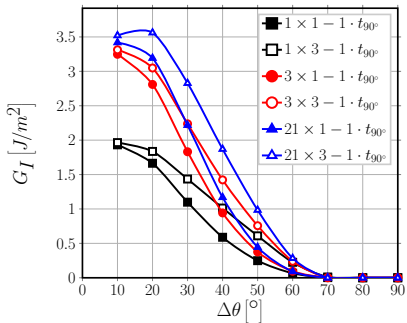
Interaction of Debonds: Strain Magnification



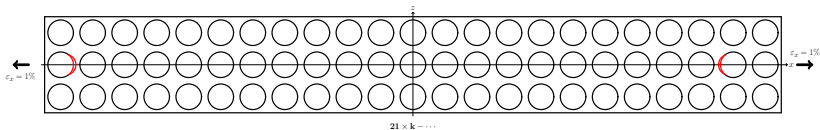
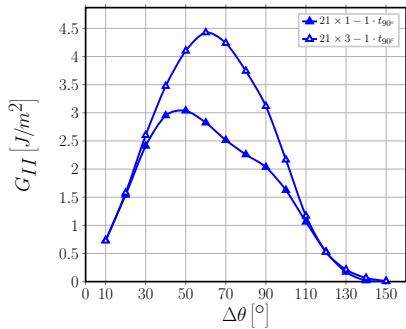
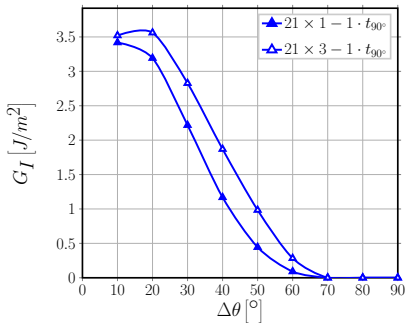
Interaction of Debonds: Strain Magnification



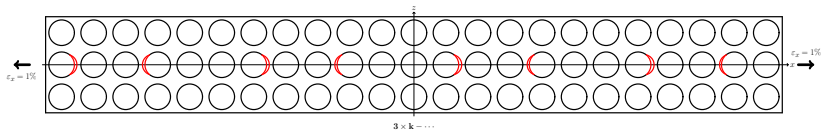
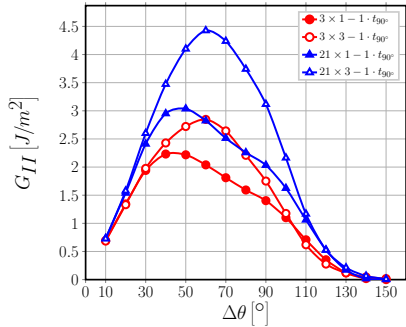
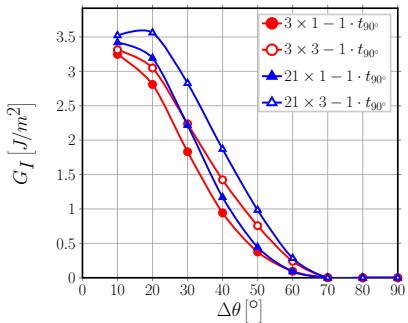
Interaction of Debonds: Strain Magnification



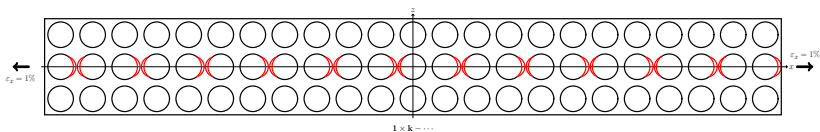
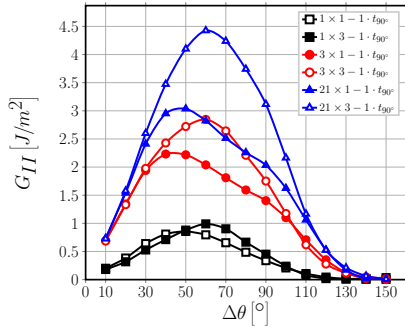
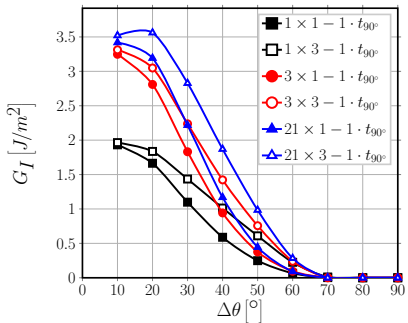
Interaction of Debonds: Crack Shielding



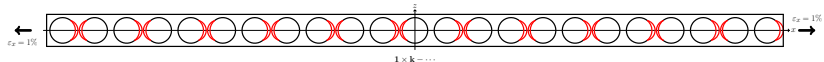
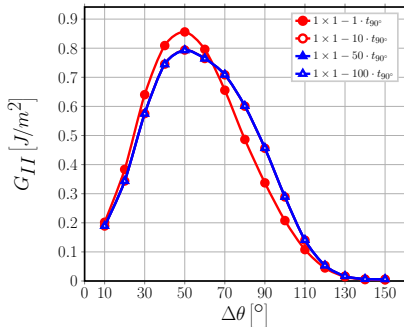
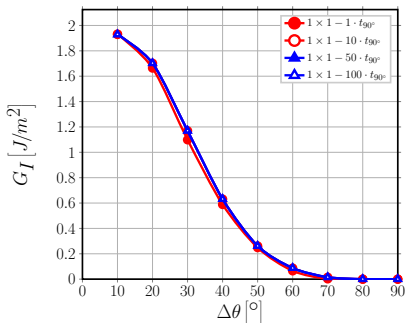
Interaction of Debonds: Crack Shielding



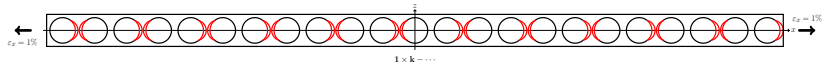
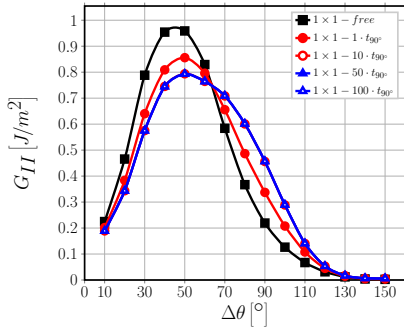
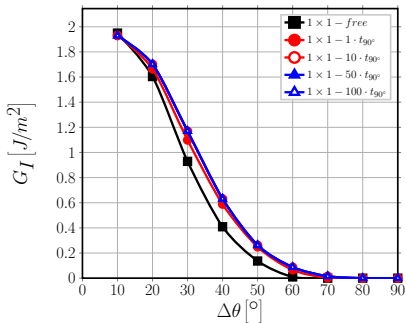
Interaction of Debonds: Crack Shielding



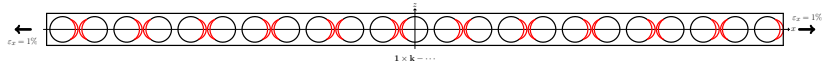
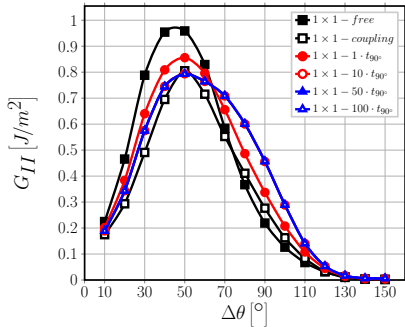
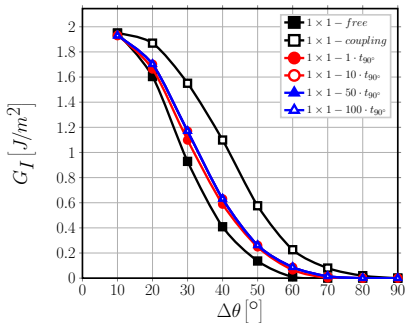
Effect of 0° ply thickness



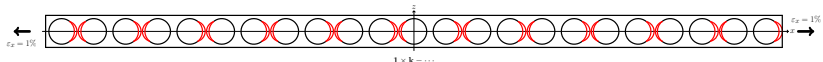
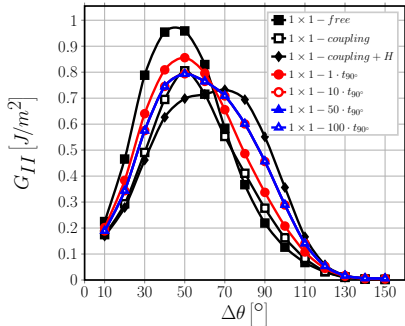
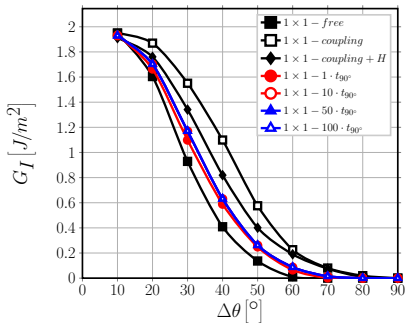
Effect of 0° ply thickness



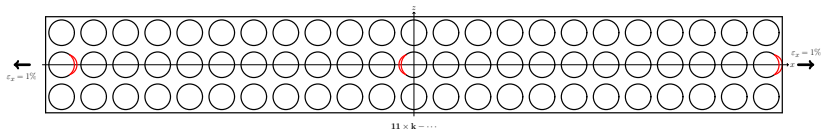
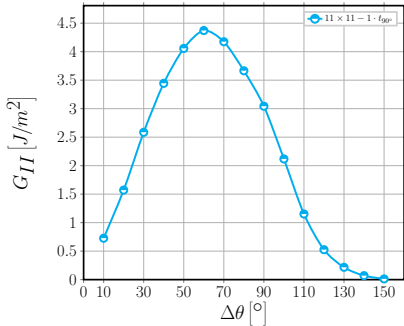
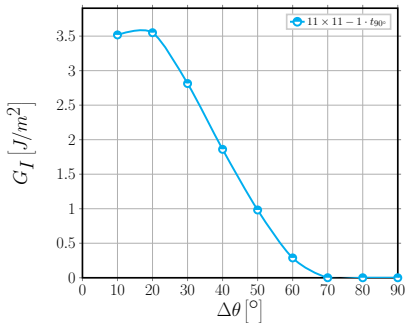
Effect of 0° ply thickness



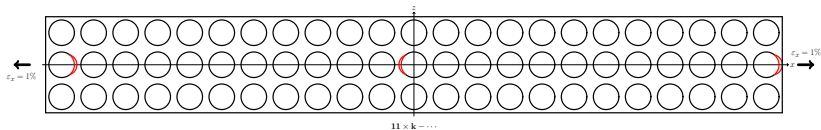
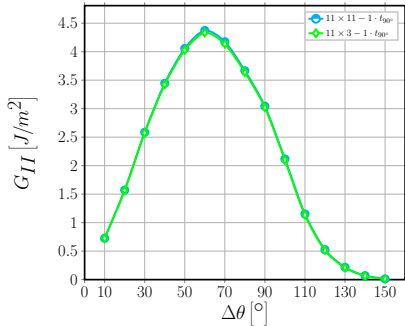
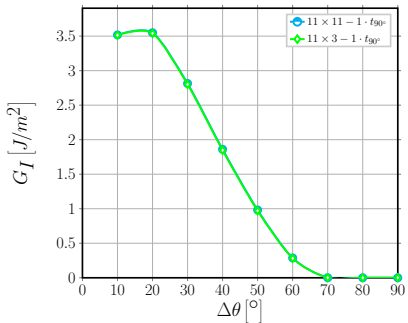
Effect of 0° ply thickness



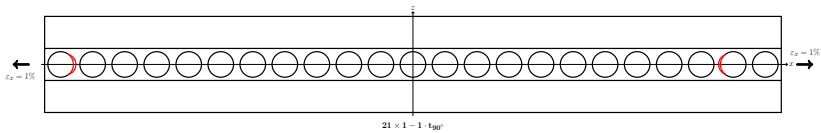
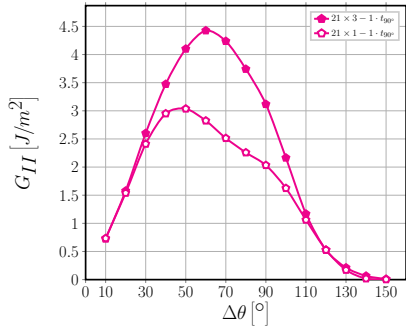
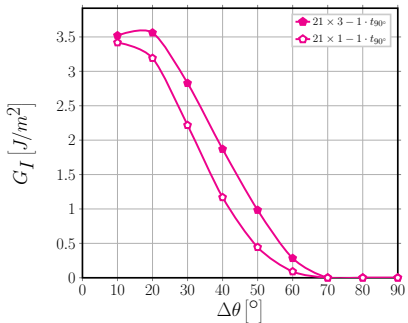
Effect of 90° ply thickness



Effect of 90° ply thickness



Effect of 90° ply thickness



Observations & Conclusions

- No effect of 90° ply thickness can be observed when t_{90° is at least $\sim 3\phi_{fiber}$
- Only if t_{90° is reduced to $1\phi_{fiber}$, ERR is reduced for a given level of applied strain, i.e. debond growth is delayed to higher levels of applied strain ($G \sim \varepsilon_{applied}^2$)
- No effect of 0° ply thickness can be observed when $t_{0^\circ}/t_{90^\circ} > 1$
- A small difference can be observed when $t_{0^\circ} = t_{90^\circ}$, due to the smaller bending stiffness of a thinner 0° layer

It seems reasonable to conclude that...

...the ply-thickness and ply-block effects have no influence on fiber/matrix interface crack growth.

Transverse Cracks Initiation Modeling Convergence Debond Initiation Debond Propagation

Interaction of Debonds Effect of 0° ply thickness Effect of 90° ply thickness Observations & Conclusions

Thank you for listening today!



LULEÅ
UNIVERSITY
OF TECHNOLOGY



Education and Culture

Erasmus Mundus